

# Disorder driven maximum in the magnetoresistance of spin polaron systems

Tanmoy Mondal<sup>1</sup> and Pinaki Majumdar<sup>2</sup>

<sup>1</sup> Harish-Chandra Research Institute (A CI of Homi Bhabha National Institute), Chhatnag Road, Jhusi, Allahabad, India 211019

<sup>2</sup> School of Arts and Sciences, Ahmedabad University, Navrangpura, Ahmedabad, India 380009

(Dated: December 29, 2025)

Ferromagnetic polarons are self trapped states of an electron in a locally spin polarised environment. They occur close to the magnetic  $T_c$  in low carrier density local moment magnets when the electron-spin coupling is comparable to the hopping scale. In non disordered systems the primary signatures are a modest non-monotonicity in the temperature dependent resistivity  $\rho(T)$ , and a magnetoresistance that can be  $\sim 20 - 30\%$  at  $T_c$ , at fields that, in energy units, are  $\sim 0.01k_B T_c$ . We find that structural disorder, in the form of pinning centers, promotes polaron formation, hugely increases the resistivity peak at  $T_c$ , and can enhance the magnetoresistance to  $\sim 80\%$ . The change in magnetoresistance with disorder is, however, non-monotonic. Too much disorder just creates an Anderson insulator - with the resistivity unresponsive to the magnetisation. This paper establishes the optimum disorder for maximising the magnetoresistance, suggests the physical process behind the unusual disorder dependence, and provides a magnetoresistance map - in terms of coupling and disorder - that locates some of the existing magnetic semiconductors within this framework.

## I. INTRODUCTION

An itinerant electron coupled to the background spins in a local moment ferromagnet can self-trap as the magnetic disorder increases with increase in temperature. The electron spin acts as a magnetic field on the background moments and, under restricted conditions, can create a polarised neighbourhood whose ‘potential well’ traps the electron. This self-trapped state is a ferromagnetic polaron (FP), the outcome of a competition between internal energy gain and entropy loss [1–6]. The state does not form if the electron-spin coupling is below a threshold, or if the electron density is not sufficiently low, or if the temperature is too low (in which the moments are anyway parallel) - or if it is too high (in which case entropy wins). The FP is an elusive object in the parameter space.

The concept of magnetic polaron originated in the 1960s in the context of Eu-based magnetic semiconductors [1, 2, 7], and has since been invoked to explain unusual transport behaviour in a broad class of low-carrier-density local-moment ferromagnets. The key signature of FP formation is the non-monotonic temperature dependence of the resistivity  $\rho(T)$  - the conventional magnetic scattering induced rise and saturation of  $\rho(T)$  across  $T_c$  is replaced by a peak near  $T_c$ , followed by an extended regime with  $d\rho/dT < 0$ . Such nonmonotonic resistivity has been observed in a variety of low carrier density local moment ferromagnets [3–10].

Most of the ferromagnetic semiconductors having polaronic features, e.g., EuO, GdN etc, are highly prone to defects. Defects generated intrinsically, or introduced through doping, act as centres for electron trapping [11–19]. The prominent features of these disordered materials are, (i) a dramatic variation in the resistivity from sample to sample, with the low temperature resistivity ranging from  $10^{-5}$  to  $10^{-3}$   $\Omega\text{cm}$ , (ii) a peak in resistivity near  $T_c$  that spans several orders of magnitude, from  $10^{-3}$  to  $10 \Omega\text{cm}$ . This wide variation is believed to be caused by changes in disorder strength, impurity concentration, and electron density [11–17, 20–24]. The variation in the resistivity peak at  $T_c$  correlates with the size of the magnetoresistance (MR) [25–27].

On the theory side there are some works that show that in

the clean limit above a critical electron-spin coupling ( $J'_c$ ) and below a critical electron density ( $n_c$ ), polarons can form [28–35], and these polaronic features are enhanced in the presence of impurities [36–44]. However, several open questions remain to be answered. For example, (i) are the effects of electron-spin coupling and structural disorder additive on the resistivity (Mathiessen’s rule)? (ii) can disorder induce polaron formation when the clean problem does not support polarons? (iii) how does disorder affect the magnetoresistance? While it is obvious that too much disorder will make the transport insensitive to magnetic order, and hence an applied field, the behaviour at moderate disorder remains unknown. Clarifying this is the central object of this paper.

The questions above are difficult to address because self-trapping occurs at finite-temperature, in a spatially correlated spin background, and involves strong electron–spin coupling where analytical approaches are inadequate. Numerical simulations, in turn, are constrained by the need to treat both thermal spin fluctuations and the electronic sector accurately, which limit the accessible system size, and the inclusion of disorder adds another layer of complexity.

Avoiding too much material specificity for the moment, in terms of band structure, etc, we study the ‘minimal model’ of a lattice of Heisenberg spins with ferromagnetic coupling  $J$ , with the spins “Kondo coupled” to itinerant electrons with coupling  $J'$  [28–35, 44]. The electrons have a tight-binding hopping  $t$  and experience an attractive potential  $-V$  at a fraction of sites.

While the effect of the ‘quenched’ impurity potential can be readily handled numerically, the difficulty is in computing the effect of the electrons on the core spins. We use a Langevin dynamics (LD) scheme [34, 35, 44–47] to treat thermal fluctuation of the spins, with an exact diagonalisation method to compute the torque. An alternate Monte Carlo approach to these models has typically been limited to size  $\sim 10 \times 10$ , but the parallelised LD approach can access lattices with  $N \sim 20 \times 20$ . This size, though still modest, allows us to study a finite concentration of polarons and map their transport, spatial, and spectral features.

In this paper, we fix the electron-spin coupling, the impurity

density, and the electron density and vary only the strength of the impurity potential  $V$ . We study the temperature dependence of physical properties for a range of  $V$  values, and the magnetic response near  $T_c$ . Our results are in a two dimensional system, we have commented on the dimension dependence elsewhere. Our main results are the following:

1. Increase in  $V$  leads to a rapid increase in the resistivity peak at  $T_c$ , but also progressively insulating behaviour at both low and high  $T$ . The fraction of resistivity arising from the interplay of structural disorder and magnetic scattering, however, first increases and then decreases with  $V$ .
2. The magnetoresistance at  $T_c$ , for a fixed field, initially grows with increasing  $V$ , peaks at some  $V_{opt}$  and then decreases again. The maximum magnetoresistance, at  $h \sim 0.1T_c$ , can be  $\sim 90\%$ .
3. A pseudogap develops at weak disorder and deepens with increasing disorder, but is suppressed by a magnetic field; at stronger disorder, disorder-induced localisation dominates, leading to a field-independent gap.
4. The resistivity can be understood from the character of electronic states close to the chemical potential. At weak disorder, the electronic states at energy  $\epsilon \lesssim \mu$  are delocalised at all  $T$ . For  $V \sim V_{opt}$  the mobility edge crosses  $\mu$  as  $T \rightarrow T_c$ . This ‘insulating’ system can be metallised by an applied field. At large  $V$  the mobility edge is well above  $\mu$  at all  $T$  and a field cannot cause a transition. The large MR is a field driven insulator-metal transition.
5. We constructed a ‘magnetoresistance map’ in terms of coupling  $J'$  and potential  $V$  to delineate the transport regimes and tentatively locate experimental samples within this scheme. We find, remarkably, that  $V_{opt} \approx 2t$  and is only weakly dependent on  $J'$ .

## II. MODEL AND METHOD

We study the Heisenberg-Kondo (H-K) model in 2D with disorder as impurity sites as:

$$H = -t \sum_{\langle ij \rangle, \sigma} c_{i\sigma}^\dagger c_{j\sigma} - J' \sum_i \mathbf{S}_i \cdot \vec{\sigma}_i - J \sum_{\langle ij \rangle} \mathbf{S}_i \cdot \mathbf{S}_j + \sum_i V_i n_i \quad (1)$$

We set the potential  $V_i = V$  on a fraction  $n_{imp}$  of randomly chosen lattice sites and zero elsewhere. We set  $t = 1$ ,  $J = 0.01t$ , electron density  $n_{el} = 0.025$  and  $n_{imp} = 0.02$ . We varied  $V$  in the range  $0.5t \leq V \leq 4.0t$ . To generate equilibrium spin configurations  $\{\mathbf{S}_i\}$  we use a LE where the spins experience a torque (below) derived from  $H$  alongside a stochastic kick, with variance  $\propto k_B T$ , to model the effect of temperature. The LE has the form:

$$\frac{d\mathbf{S}_i}{dt} = \mathbf{S}_i \times (\mathbf{T}_i + \mathbf{h}_i) - \gamma \mathbf{S}_i \times (\mathbf{S}_i \times \mathbf{T}_i)$$

$$\begin{aligned} \mathbf{T}_i &= -\frac{\partial H}{\partial \mathbf{S}_i} = -J' \langle \vec{\sigma}_i \rangle - J \sum_{\delta} \mathbf{S}_j \delta_{j,i+\delta} \\ \langle h_{i\alpha} \rangle &= 0, \quad \langle h_{i\alpha}(t) h_{j\beta}(t') \rangle = 2\gamma k_B T \delta_{ij} \delta_{\alpha\beta} \delta(t - t') \end{aligned} \quad (2)$$

$\mathbf{T}_i$  is the effective torque acting on the  $i$ -th site,  $\gamma = 0.1$  is a damping constant, and  $\mathbf{h}_i$  is the thermal noise satisfying the fluctuation-dissipation theorem.  $\langle \vec{\sigma}_i \rangle$  represents the expectation of  $\vec{\sigma}_i$  taken over the instantaneous ground state of the electrons, and  $\delta$  is the set of nearest neighbours. In the presence of an external magnetic field there is an additional term  $\hat{z}h$  in  $\mathbf{T}_i$ . Once Langevin evolution reaches equilibrium the magnetic correlations can be computed from the  $\{\mathbf{S}_i\}$ , and electronic features obtained by diagonalisation in these backgrounds.

## III. RESULTS AT ZERO FIELD

Fig.1(a) shows  $\rho(T)$  for different  $V$ . For  $V = t$  the non-monotonic behaviour of near  $T_c$  is enhanced compared to a clean system [34, 35]. A disorder-driven insulating tendency appears as  $T \rightarrow 0$ , but this feature is not related to polaronic physics. For  $V = 2t$ , the nonmonotonicity near  $T_c$  is further amplified. The combined influence of  $V$  and  $J'$  is not a simple addition of their individual effects; rather, the system responds in a strongly intertwined and nonlinear manner. Moreover, a pronounced insulating behaviour emerges as  $T \rightarrow 0$ , with a much stronger insulating character than in the  $V = t$  case. If the disorder strength is increased further, the electrons become strongly trapped around the impurity sites, and insensitive to the magnetic background. As a result, the polaronic effect is progressively diminished. The strong localisation around impurities leads to an insulating  $\rho(T)$  behaviour at all  $T$ , with  $\rho(T)$  determined mainly by  $V$ .

We define the resistivity  $\rho_{cr}(T)$  that arises from the cross

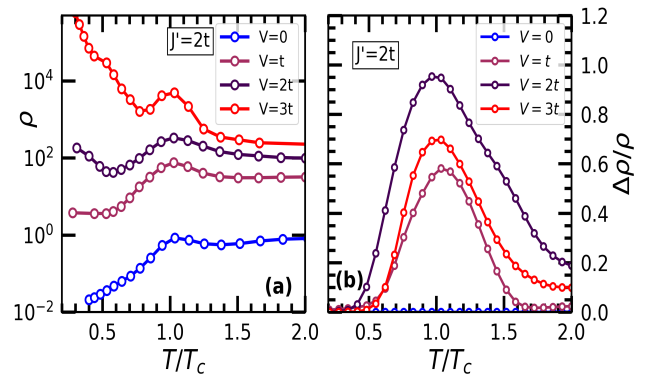


FIG. 1. The zero field resistivity  $\rho(T)$ . (a) The resistivity at  $V = 0$  and three finite values of  $V$ . Note the maxima-minima structure in  $\rho(T)$  and the increasing insulating behavior at low and high temperature as  $V$  increases. (b) The ‘cross term’  $\rho_{cr}(T)$  (see text) normalised by  $\rho(T)$ . This captures the enhancement due to the coupling of structural and magnetic effects. This function grows initially with increasing  $V$ , and drops after  $V = 2t$ .

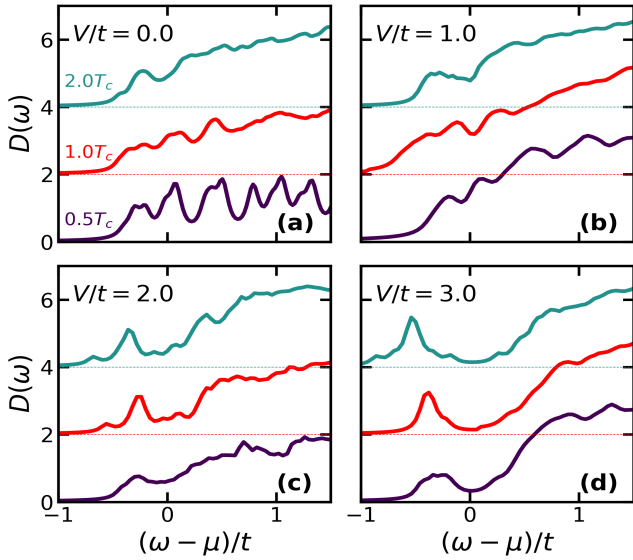


FIG. 2. Density of states at zero field. Panels (a)-(d) show the DOS for  $V/t = 0, 1, 2, 3$ , respectively, for three values of  $T/T_c$  (marked in panel (a)). Other panels follow the same colour code. At  $V = 0$  there is essentially featureless at all  $T$ , with the finite size fluctuations smoothing out with  $T$ . At  $V/t = 1, 2$  we see a depression (pseudogap) appearing around  $\omega \sim \mu$  with increasing  $T$ . At  $V = 3t$  there is a prominent depression already at  $T = 0$  and it becomes somewhat broader at persists to the highest  $T$ . We are approaching a regime where the DOS is ‘gapped’ and essentially  $T$  independent.

coupling of impurity and magnetic effects as below:

$$\rho(T) = \rho_V(T) + \rho_{J'}(T) + \rho_{cr}(T)$$

where  $\rho(T)$  is the full resistivity,  $\rho_V(T)$  is the resistivity with  $V$  acting alone, and  $\rho_{J'}(T)$  is the resistivity of the clean magnetic system.  $\rho_{cr}(T)$  then encodes the enhancement of resistivity due to the ‘interference’ of structural and magnetic effects. And, it is this ‘extra’ that can be affected by a magnetic field to generate a MR that is bigger than in the clean system. Fig.1(b) shows the behaviour of  $\rho_{cr}(T)/\rho(T)$  for three values of  $V$ . By definition, this object is zero at  $V = 0$ .

We now examine how this enhanced polaron formation influences the DOS. Fig.2 shows the effect of varying  $V$  and  $T$  at  $J' = 2t$  on the DOS. Panel (a) shows the non disordered case for reference. At  $V = t$  a faint pseudogap appears at the Fermi energy. This reflects the strengthening of electron localisation and the formation of stronger FPs, which generate bound states near the lower edge of the DOS. At  $V = 2t$ , the pseudogap deepens and becomes more pronounced. By  $V = 3t$ , a clear gap emerges. In this strong-disorder limit, the FP picture becomes less relevant: electron motion is dominated by disorder-induced localisation, which governs the system’s behaviour more strongly than polaronic effects.

#### IV. EFFECT OF A MAGNETIC FIELD

Upto now, we have talked about the zero field resistivity. Now we discuss the effect of applied field. Application of a magnetic field aligns the localised spins toward ferromagnetic order, thereby suppressing the nonmonotonic behaviour of  $\rho(T)$ . For sufficiently large fields, the background spins become fully ferromagnetically aligned, and the nonmonotonicity is completely removed and which gives rise to colossal MR. So, the stronger the nonmonotonicity the larger the MR. The MR can be quantified through the ratio  $(\rho(T_c, h = 0) - \rho(T_c, h)) / \rho(T_c, h = 0)$ . However, a simplified estimate of MR can be obtained by replacing  $h$  with  $h_c$ , where  $h_c$  denotes the field strength required to eliminate the nonmonotonicity. In practice, this can be estimated more conveniently by assuming a fully ferromagnetic spin background, effectively replacing  $h_c$  with  $h_{\inf}$ .

Fig.3(a) shows the effect of  $V$  and  $h$  on  $\Delta\rho$  at  $J' = 2t$ . For a fixed  $h$ ,  $\Delta\rho$  initially increases with disorder strength  $V$ , reaches a maximum at a characteristic value  $V_{opt}$ , and subsequently decreases. This behaviour arises because, at low and intermediate disorder, the nonmonotonicity of  $\rho(T)$  strengthens with increasing  $V$ , enhancing the polaronic contribution to MR. Beyond  $V_{opt}$ , however, strong disorder progressively lessens the influence of the magnetic background, suppressing polaronic features and thereby reducing MR. As expected, the magnitude of the MR depends strongly on  $h$ , showing a 75% increase as the field is increased from  $0.001t$  to  $0.01t$ .

Figure 3(b) shows the  $J'$  dependence of MR estimated within the high-field calculation. The MR increases gradually with increasing  $J'$ , as expected from the corresponding enhancement of the nonmonotonicity with  $J'$ . Although the

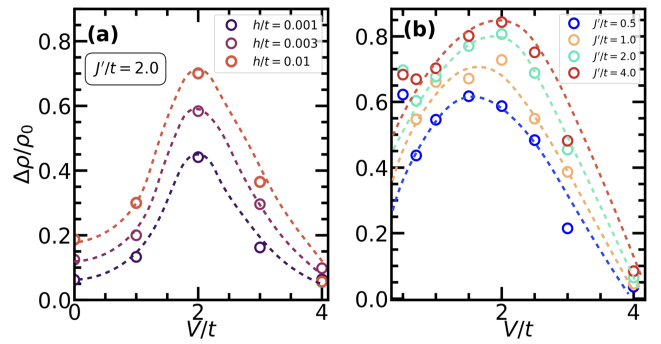


FIG. 3. Magnetoresistance. (a) The MR, defined as  $(\rho(T, 0) - \rho(T, h)) / \rho(T, 0)$  at  $T = T_c$  and  $h/t = 0.001, 0.003, 0.01$  shown for varying  $V$ . The MR expectedly increases with increasing  $h$ , but has an unusual  $V$  dependence. The moderate MR,  $\sim 10 - 20\%$  at  $V = 0$  increases to a maximum  $\sim 60 - 70\%$  at  $V \sim 2t$ , and then falls off. (b) The high temperature, high field, MR -  $(\Delta\rho/\rho)_\infty$  - where  $\rho$  is the resistivity is the background of the structural disorder and random spins, and the suppression corresponds to a fully spin-polarised background. This calculation does not involve any magnetic annealing. We want to highlight that this quantity is a reasonable proxy for the finite  $T$ , finite  $h$  MR both in terms of magnitude and  $V$  dependence.

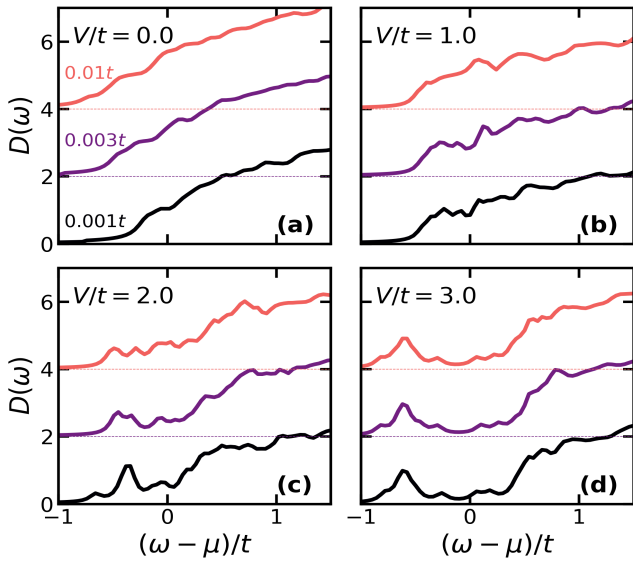


FIG. 4. Field dependence of the density of states. The panels (a)-(d) show the DOS at  $T = T_c$  for  $h/t = 0.001, 0.003, 0.01$  and  $V/t = 0, 1, 2, 3$ . (a) At  $V = 0$  the DOS is essentially featureless and insensitive to  $h$ . (b)-(c) The modest dip at  $\omega \sim \mu$  at  $h = 0$  is smoothed out with increasing  $h$ . For  $V = 2t$  the low  $h$  dip is more prominent than at  $V = t$ . (d) The prominent suppression in the DOS near  $\mu$  at  $T_c$  is hardly affected by application of the field.

rate of increase slows down at larger  $J'$ . The location of  $V_{opt}$  exhibits only a weak dependence on  $h$ .

We now discuss the effect of a magnetic field on the DOS for different values of  $V$  at  $T = T_c$ , as shown in Fig. 4. In the absence of disorder [panel (a)], no pseudogap-like feature is present, and consequently, the effect of the magnetic field is unobservable. In contrast, for stronger disorder, where a pseudogap develops at the Fermi level at  $h = 0$ , the application of a magnetic field suppresses the gap, as seen for  $V = t$  and  $2t$ . This behaviour indicates the suppression of polaronic effects with increasing  $h$ . However, for  $V = 3t$ , the gap remains essentially unaffected by the field. In this strong-disorder limit, the influence of localised spins becomes much less significant, rendering the FP picture less relevant.

## V. INSULATOR-METAL TRANSITION SCENARIO

We now try to identify the basic mechanism behind the transport and spectral response of the system and frame it in a familiar language. There are no electron-electron interactions in our model and the physics can be understood in terms of the single particle eigenstates, albeit in complex, annealed, background configurations  $\{V_i, S_i\}$ . While the  $V_i$  are specified, the  $\{S_i\}$  distribution depends on the  $V_i$  as also  $T$  and  $h$ .

As the spin distribution evolves from its  $T = 0$  full polarisation, through the  $T \sim T_c$  locally polarised configurations, to the random  $T \gg T_c$  state, the mobility edge shifts with  $T$ . At  $T = 0$  the electrons are subject only to structural disorder, and ideally in the 2D geometry where we are studying

the problem all states in the band would be localised. We are however considering only states with localisation length  $\ll L$ , to mimic what one would see in 3D. With this caveat, the mobility edge  $\epsilon_c$  starts below  $\mu$  at small  $V$  and low  $T$  and moves up as  $T$  increases. At weak  $V$  it does not cross  $\mu$  at any  $T$ , approaching it closest near  $T_c$ , Fig.5(a).

We see enhanced scattering, and a peak in resistivity, but no ‘localisation’ of states at  $\mu$  even at  $T_c$  for  $V = 0, t$ . At  $V = 2t$  however the interplay of  $V_i$  and polaron formation leads to  $\epsilon_c$  crossing  $\mu$  near  $T = T_c$ . Nominally we would have a mobility gap but the finite  $T$  leads to a finite conductivity. At  $V = 3t$ , however,  $\epsilon_c$  is above  $\mu$  at all  $T$  and the chemical potential is in the region of localised states. We have an insulator with  $t$  dependent mobility gap. On the whole, the scenario we propose (modulo 2D weak localisation effects) is that both structural disorder and thermally induced polaron formation can drive a metal-insulator transition in the system.

Fig.5(b), where we consider the field dependence of  $\epsilon_c - \mu$  at  $T = T_c$ , is just the reverse. Now at  $V = 0, t$ , the mobility edge is pushed below, towards the lower band edge as  $h$  increases, making the states near  $\mu$  more conducting. At  $V = 2t$ , where the  $h = 0$  mobility edge was above  $\mu$  we see that a small field can push  $\epsilon_c$  below  $\mu$ . This would now be a field driven insulator-metal transition, a complement of the thermally driven metal-insulator transition. We see echoes of manganite physics but with very different microscopic ingredients. At  $V = 3t$  there is an effect similar to what we see at

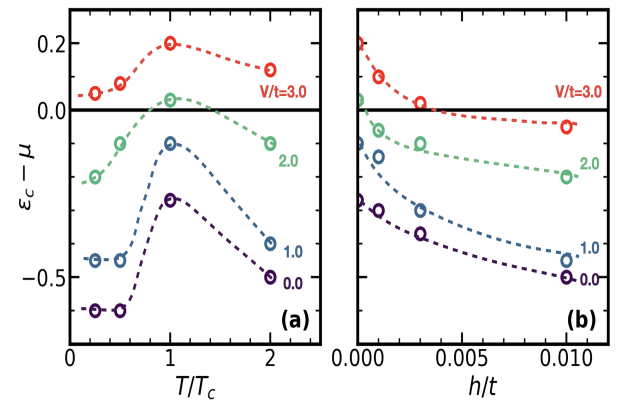


FIG. 5. Location of the mobility edge  $\epsilon_c$  with respect to the chemical potential. The mobility edge is calculated via an estimate of the inverse participation ratio (IPR) of the electronic states on the annealed backgrounds. (a) Shows the temperature dependence of  $\epsilon_c - \mu$  at  $h = 0$  for  $V/t = 0, 1, 2, 3$ . For  $V/t = 0, 1$  the mobility edge approaches  $\mu$  from below, comes closest for  $T \sim T_c$ , but never crosses. The states are always delocalised. At  $V = 2t$  it crosses near  $T = T_c$  and drops back again. For  $V = 3t$   $\epsilon_c - \mu > 0$  for all  $T$ , the states at the chemical potential are always localised. (b) This tracks the field dependence of  $\epsilon_c - \mu$  staying at  $T = T_c$ . The applied field expectedly drives the mobility edge downwards since it weakens localisation. From the data we see that at  $V = 2t$  a weak field can push  $\epsilon_c$  from above  $\mu$  to below  $\mu$ , crudely causing an ‘insulator-metal transition’. Something similar happens at  $V = 3t$  as well, but at much larger field. At even larger  $V$  the insulating state will persist at arbitrarily large  $h$ .

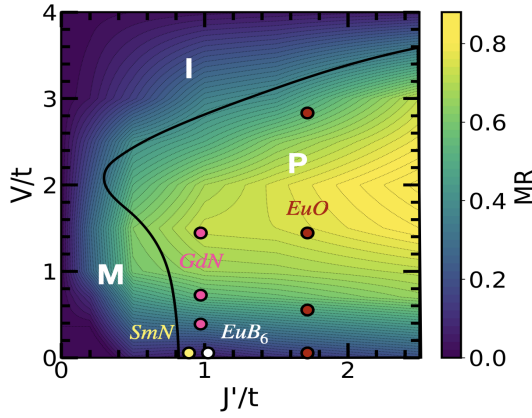


FIG. 6. Map of magnetoresistance. This panel shows a surface plot of the ‘magnetoresistance’ ( $\Delta\rho/\rho\omega_\infty$ , which, we have demonstrated, is a good mimic of the fully annealed result. At a typical  $J'$  increasing  $V$  leads to an increase in MR and then a fall. The optimal disorder is  $V \sim 2t$ , slowly increasing with  $J'$ . The firm black line separates the polaronic regime (P), where we have a peak-dip structure in  $\rho(T)$ , from the simple metallic (M) or insulating (I) regimes.

$V = 2t$ , but now at a much higher field. At even larger  $V$  we surmise that even very large  $h$  would not be able to change the insulating character.

This analysis provides a pointer to the  $V_{opt}$  that maximises the MR. We need a  $V$  such that at  $h = 0$  the mobility edge just crosses  $\mu$  for  $T \sim T_c$ . In that case a weak field will be able to push it below  $\mu$ , create an insulator-metal transition, and generate large MR. At  $V < V_{opt}$  the mobility edge never crosses  $\mu$ , for  $V \gg V_{opt}$  the mobility edge cannot be pushed down below  $\mu$ .

## VI. PHASE DIAGRAM

While our detailed discussion has been at a ‘typical’ electron-spin coupling  $J' = 2t$ , with varying  $V$ , we would like to put forward a broader phase diagram based on an approximate calculation. Fig.6 attempts this, where, for the parameters used in this paper, but varying  $J'$  and  $V$ , we suggest a magnetoresistance map, as well as a transport regime classification.

The resistive character of the  $V - J'$  problem can be classified into the following categories, based on their trends at  $T \ll T_c$ , around  $T_c$ , and at  $T \gg T_c$ . First, the two simple regimes are: **1.** Metallic (M), i.e,  $d\rho/dT > 0$  at all  $T$ : For

$V \ll t$  and  $J' < J'_c$ ,  $\rho(T)$  is completely monotonic, with  $\rho \rightarrow 0$  as  $T \rightarrow 0$ . This regime is well established in the literature on ferromagnetic materials [48]. **2.** Insulating (I), i.e,  $d\rho/dT < 0$  at all  $T$ : At very large  $V$  the magnetic background plays no significant role. Electrons become strongly localised around impurity sites, and  $\rho(T)$  is insulating at all temperatures. The nonmonotonic feature disappears entirely, and the resistivity becomes essentially independent of  $J'$ . The M and I regimes are marked in the figure. We have not shown an Anderson transition point at  $J' = 0$  since that is not meaningful in a 2D problem. There would be such a point however in the 3D case, separating the M and I.

The complicated regime is **3.** Polaronic near  $T_c$ : For  $V \ll t$  the resistivity is metallic both for  $T \ll T_c$  and  $T \gg T_c$ , while a clear  $d\rho/dT < 0$  region appears near  $T_c$ , signaling the formation of polarons. This resembles the behaviour seen in EuB<sub>6</sub>, SmN, etc. For moderate disorder ( $2t \leq V < 4t$ ) the resistivity becomes strongly nonmonotonic. At  $T \rightarrow 0$ , it shows insulating behaviour due to impurity-driven localisation, followed by an enhanced polaronic feature near  $T_c$ , and finally a metallic saturation at  $T \gg T_c$ . Several samples of EuO, GdN, EuS and related compounds fall in this category [2, 11, 16, 17]. Upon further increasing  $V$ , the magnetic background becomes irrelevant in electronic transport. On the whole the region enclosed by the firm black line is the polaronic region where large MR is expected.

The colour code in the map corresponds to the artificial ‘infinite temperature, infinite field’ magnetoresistance that we showed in Fig.3(b), since a full annealing based calculation over  $V$  and  $J'$  is very expensive. The map reveals that the optimal  $V$  is  $\sim 2t$ , for the impurity and electron density used, and increases only slightly with  $J'$ .

## VII. CONCLUSION

In summary, we have demonstrated that moderate disorder promotes magnetic polaron formation and enhances the magnetoresistance - which can reach up to 90%. However, beyond an optimal disorder the MR starts decreasing and vanishes as  $V \rightarrow \infty$ . We trace the origin of this effect to a thermally driven metal-insulator transition that arises from polaron formation in a structurally disordered background, and the field driven metallisation of this state driving the large magnetoresistance. We provide a map of the magnetoresistance in terms of electron-spin coupling and impurity potential and locate the optimal disorder for maximising the magnetoresistance.

---

[1] R. R. Heikes and C. W. Chen, Evidence for impurity bands in La-doped EuS, *Physics Physique Fizika* **1**, 159 (1964).

[2] Y. Shapira, T. B. Reed, Resistivity and Hall Effect of EuS in Fields up to 140 kOe, *Phys. Rev. B* **5**, 4877 (1972).

[3] Molnar, S. von, Static and Dynamic Properties of the Insulator–Metal Transition in Magnetic Semiconductors, Including the Perovskites, *Journal of Superconductivity* **14**, 199–204 (2001).

[4] M Ziese, Extrinsic magnetotransport phenomena in ferromagnetic oxides, *Rep. Prog. Phys.* **65** 143 (2002).

[5] C. Lin, C. Yi, Y. Shi, L. Zhang, G. Zhang, Jens Müller, and Y. Li, Spin correlations and colossal magnetoresistance in HgCr<sub>2</sub>Se<sub>4</sub>, *Phys. Rev. B* **94**, 224404 (2016).

[6] S. Kimura, T. Nanba, S. Kunii, and T. Kasuya, Interband Optical Spectra of Rare-Earth Hexaborides, *J. Phys. Soc. Jpn.* **59**, pp. 3388-3392 (1990).

[7] S. von Molnar and S. Methfessel, *J. Appl. Phys.* **38**, 959 (1967).

[8] Z. Yang, X. Bao, S. Tan, and Y. Zhang, Magnetic polaron conduction in the colossal magnetoresistance material  $\text{Fe}_{1-x}\text{Cd}_x\text{Cr}_2\text{S}_4$ , *Phys. Rev. B* **69**, 144407 (2004).

[9] P. Das, A. Amyan, J. Brandenburg, J. Müller, P. Xiong, S. von Molnár, and Z. Fisk, Magnetically driven electronic phase separation in the semimetallic ferromagnet EuB<sub>6</sub>, *Phys. Rev. B* **86**, 184425 (2012).

[10] Li, H., Xiao, Y., Schmitz, B. et al. Possible magnetic-polaron-switched positive and negative magnetoresistance in the GdSi single crystals. *Sci Rep* **2**, 750 (2012).

[11] F. Natali, B. J. Ruck, H. J. Trodahl, Do Le Binh, S. Vezian, B. Damilano, Y. Cordier, F. Semond, and C. Meyer, Role of magnetic polarons in ferromagnetic GdN, *Phys. Rev. B* **87**, 035202 (2013).

[12] W. B. Mi; Z. B. Guo; X. F. Duan; X. J. Zhang; H. L. Bai, Large negative magnetoresistance in reactive sputtered polycrystalline GdN<sub>x</sub> films, *Appl. Phys. Lett.* **102**, 222411 (2013).

[13] A. R. H. Preston; B. J. Ruck; W. R. L. Lambrecht; L. F. J. Piper; J. E. Downes; K. E. Smith; H. J. Trodahl, Electronic band structure information of GdN extracted from x-ray absorption and emission spectroscopy, *Appl. Phys. Lett.* **96**, 032101 (2010).

[14] Peter Wachter, Physical and Chemical Properties of GdN: A Critical Comparison between Single Crystals and Thin Films, Theory and Experiment, *Advances in Materials Physics and Chemistry*, Vol.6 No.3, (2016).

[15] G. L. S. Vilela, G. M. Stephen, X. Gratens, G. D. Galgano, Yasen Hou1, Y. Takamura, D. Heiman1,3, A. B. Henriques, and G. Berera et al., Spin splitting tunable optical band gap in polycrystalline GdN thin films for spin filtering, *Phys. Rev. B* **109**, L060401 (2024).

[16] M. R. Oliver, J. O. Dimmock, A. L. McWhorter, and T. B. Reed, Conductivity Studies in Europium Oxide, *Phys. Rev. B* **5**, 1078 (1972).

[17] Y. Shapira, S. Foner, and T. B. Reed, EuO. I. Resistivity and Hall Effect in Fields up to 150 kOe *Phys. Rev. B* **8**, 2299 (1973).

[18] C. S. Snow, S. L. Cooper, D. P. Young, Z. Fisk, Arnaud Comment, and Jean-Philippe Ansermet, Magnetic polarons and the metal-semiconductor transitions in (Eu, La)B<sub>6</sub> and EuO: Raman scattering studies, *Phys. Rev. B* **64**, 174412 (2001).

[19] S. J. Blundell, T. Lancaster, F. L. Pratt, P. J. Baker, W. Hayes, J.-P. Ansermet, and A. Comment, Phase transition in the localized ferromagnet EuO probed by  $\mu$ SR *Phys. Rev. B* **81**, 092407 (2010).

[20] Shin-ichi Kimura, Takahiro Ito, Hidetoshi Miyazaki, Takafumi Mizuno, Takuya Iizuka, and Toshiharu Takahashi, Electronic inhomogeneity EuO: Possibility of magnetic polaron states, *Phys. Rev. B* **78**, 052409 (2008).

[21] P. G. Steeneken, L. H. Tjeng, I. Elfimov, G. A. Sawatzky, G. Ghiringhelli, N. B. Brookes, and D.-J. Huang, Exchange Splitting and Charge Carrier Spin Polarization in EuO, *Phys. Rev. Lett.* **88**, 047201 (2002).

[22] Wen-Yi Tong, Hang-Chen Ding, Yong-Chao Gao, Shi-Jing Gong, Xiangang Wan, and Chun-Gang Duan, Spin-dependent optical response of multiferroic EuO: First-principles DFT calculations *Phys. Rev. B* **89**, 064404 (2014).

[23] Dipta Bhanu Ghosh, Molly De, and S. K. De, Electronic structure and magneto-optical properties of magnetic semiconductors: Europium monochalcogenides, *Phys. Rev. B* **70**, 115211 (2004).

[24] S. G. Altendorf, A. Efimenko, V. Oliana, H. Kierspel, A. D. Rata, and L. H. Tjeng, Oxygen off-stoichiometry and phase separation in EuO thin films, *Phys. Rev. B* **84**, 155442 (2011).

[25] S. Süllow, I. Prasad, M. C. Aronson, S. Bogdanovich, J. L. Sarrao, and Z. Fisk, Metallization and magnetic order in EuB<sub>6</sub>, *Phys. Rev. B* **62**, 11626 (2000).

[26] X. Zhang, L. Yu, S. von Molnár, Z. Fisk, and P. Xiong, Non-linear Hall Effect as a Signature of Electronic Phase Separation in the Semimetallic Ferromagnet EuB<sub>6</sub>, *Phys. Rev. Lett.* **103**, 106602 (2009).

[27] M. Pohlit, S. Rößler, Y. Ohno, H. Ohno, S. von Molnár, Z. Fisk, J. Müller, and S. Wirth, Evidence for Ferromagnetic Clusters in the Colossal-Magnetoresistance Material EuB<sub>6</sub>, *Phys. Rev. Lett.* **120**, 257201 (2018).

[28] P. Majumdar and P. Littlewood, Magnetoresistance in Mn Pyrochlore: Electrical Transport in a Low Carrier Density Ferromagnet, *Phys. Rev. Lett.* **81**, 1314 (1998).

[29] M. J. Calderón, L. Brey, and P. B. Littlewood, Stability and dynamics of free magnetic polarons, *Phys. Rev. B* **62**, 3368 (2000).

[30] L. G. L. Wegener and P. B. Littlewood, Fluctuation-induced hopping and spin-polaron transport, *Phys. Rev. B* **66**, 224402 (2002).

[31] Tao Liu, Mang Feng, Kelin Wang, A variational study of the self-trapped magnetic polaron formation in double-exchange model, *Physics Letters A*, Volume 337, Issues 4–6, 2005.

[32] L. Craco, C. I. Ventura, A. N. Yaresko, and E. Müller-Hartmann, Mott-Hubbard quantum criticality in paramagnetic CMR pyrochlores, *Phys. Rev. B* **73**, 094432 (2006).

[33] M. J. Calderón, L. G. L. Wegener, and P. B. Littlewood, Evaluation of evidence for magnetic polarons in EuB<sub>6</sub>, *Phys. Rev. B* **70**, 092408 (2004).

[34] Tanmoy Mondal, Pinaki Majumdar, Inhomogeneous tunneling, nonmonotonic resistivity, and non-Drude optics in EuB<sub>6</sub>, *Phys. Rev. B* **111**, 195103 (2025).

[35] Tanmoy Mondal, Pinaki Majumdar, Crossover from self-trapped bound states to perturbative scattering in the Heisenberg-Kondo lattice model, arXiv:2510.24520

[36] J. Spalek, M. Lubecka, and A. Werzyn, Carrier Concentration and Magnetic Susceptibility of Doped Ferromagnetic Semiconductors with Application to EuO: Eu, *phys. stat. sol. (b)*, **82**: 107-116 (1977).

[37] P. Kuivalainen, J. Sinkkonen, K. Kaski, and T. Stubb, Bound magnetic polaron in magnetic semiconductors, *phys. stat. sol. (b)*, **94**: 181-190 (1979).

[38] A. Mauger, Magnetic polaron: Theory and experiment, *Phys. Rev. B* **27**, 2308 (1983).

[39] P. Sinjukow and W. Nolting, Metal-insulator transition in EuO, *Phys. Rev. B* **68**, 125107 (2003).

[40] P. Sinjukow and W. Nolting, Fully self-consistent determination of transport properties in Eu-rich EuO, *Phys. Rev. B* **69**, 214432 (2004).

[41] Michael Arnold and Johann Kroha, Simultaneous Ferromagnetic Metal-Semiconductor Transition in Electron-Doped EuO, *Phys. Rev. Lett.* **100**, 046404 (2008).

[42] Tobias Stollenwerk and Johann Kroha, Theory of Curie temperature enhancement in electron-doped EuO, *Phys. Rev. B* **92**, 205119 (2015).

[43] Henryk Bednarski and Józef Spałek, Effect of thermodynamic fluctuations of magnetization on the bound magnetic polaron state in ferromagnetic semiconductors, *New J. Phys.* **16** 093060 (2014).

[44] Tanmoy Mondal, Pinaki Majumdar, Disorder enhanced ferromagnetic polaron formation—and the test case of Europium Ox-

ide, arXiv:2506.14001

[45] Pui-Wai Ma and S. L. Dudarev, Langevin spin dynamics, *Phys. Rev. B* **83**, 134418 (2011).

[46] P.-W. Ma and S. L. Dudarev, *Phys. Rev. B* **86**, 054416 (2012).

[47] Gia-Wei Chern, Kipton Barros, Zhentao Wang, Hidemaro Suwa, and Cristian D. Batista, Semiclassical dynamics of spin density waves, *Phys. Rev. B* **97**, 035120 (2018).

[48] Michael E. Fisher and J. S. Langer. Resistive Anomalies at Magnetic Critical Points, *Phys. Rev. Lett.* **20**, 665 (1968).